Plasma Chemistry and Plasma Processing, Vol. 13, No. 1, 1993

Pulverized Coal Plasma Gasification

R. A. Kalinenko,[1,3] A. P. Kuznetsov,[1] A. A. Levitsky,[1] V. E. Messerle,[2] Yu. A. Mirokhin,[1] L. S. Polak,[1] Z. B. Sakipov,[2] and A. B. Ustimenko[2]

Received July 20, 1991; revised April 1, 1992

A number of experiments on the plasma-vapor gasification of brown coals of three types have been carried out using an experimental plant with an electric-arc reactor of the combined type. On the basis of the material and heat balances, process parameters have been obtained: the degree of carbon gasification (ξ_c), the level of sulfur conversion into the gas phase (ξ_s), the synthesis gas concentration ($CO+H_2$) in the gaseous products, and the specific power consumption for the gasification process. The degree of gasification was 90.5–95.0%, the concentration of the synthesis gas amounted to 84.7–85.7%, and the level of sulfur conversion into the gas phase was 94.3–96.7%. Numerical study of the process of plasma gasification of coals was carried out using a mathematical model of motion, heating, and gasification of polydisperse coal particles in an electric-arc reactor of the combined type with an internal heat source (arc). The initial conditions for a conjugate system of nonlinear differential equations of the gas dynamics and kinetics of a pulverized coal stream interacting with the electric arc and oxidizer (water vapor) agree with the initial conditions of the experiments. The computation results satisfactorily correlate with the experimental data. The mathematical model can be used for the determination of reagent residence time and geometrical dimensions of the plasma reactor for the gasification of coals.

KEY WORDS: Plasma gasification; lower-grade coals; electric-arc reactor; mathematical model of plasma gasification of coals.

1. INTRODUCTION

A marked tendency in the past decade to a more rapid increase in the price of fossil energy sources (gas, oil, coal), and that of electric power, has created the need to develop new methods for production of chemicals which consume less combustible minerals and more electric power, as

[1]Institute of Petrochemical Synthesis, Russian Academy of Sciences, 29 Leninskii Prospect, 117071 Moscow, Russia.
[2]Kazakh Research Institute of Power Engineering, Alma-Ata, Kazakhstan.
[3]To whom correspondence should be addressed.

0272-4324/93/0300-0141$07.00/0

compared with conventional processes. These are, first of all, processes based on the use of plasma: production of acetylene by pyrolysis of hydrocarbon gases, oil fractions, and coal in hydrogen plasma,[1,2] and production of synthesis gas by gasification of hydrocarbon raw stocks in water vapor plasma or a vapor-oxygen mixture.[3,5] In the latter case any fuel can, in practice, be used as raw material, such as coal of different degrees of metamorphism, peat, biomass, petroleum, and natural gas.

The new process and its equipment are now being intensively studied. Mathematical models and computation of optimal process parameters may play a great role in the development of plasma-chemical methods of processing hydrocarbon raw material.

The present article reports the results of coal gasification experiments with water vapor in an original plasma reactor (with combined heat release and absorption zones) and presents a mathematical model describing a two-phase reacting stream. The results of the experiments are compared with the calculated data.

2. EXPERIMENTAL

2.1. Description of Experimental Plant

The experimental plant used for the plasma conversion of coals (Fig. 1a)[6] consists of a three-phase plasma generator-reactor 1,[7] slag catcher

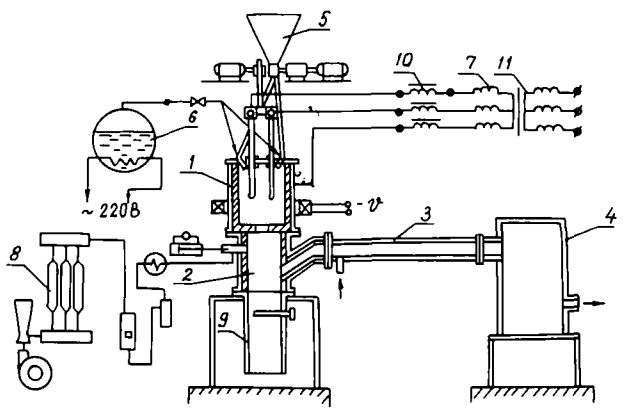

Fig. 1a. Experimental apparatus for the plasma conversion of coals: 1, reactor; 2, gas and slag separation chamber; 3, synthesis-gas oxidation chamber; 4, cooling chamber; 5, star dust feeder; 6, hot-water boiler; 7, power supply unit; 8, gas analysis system; 9, slag catcher; 10, choke; 11, transformer.

2, synthesis-gas oxidation chamber 3, cooling chamber 4, coal pulverization and feeding system 5, steam feeding system 6, electric-power supply unit 7, instrumentation complex, water cooling, and influx-exhaust ventilation system.

The plasma generator-reactor 1, of adjustable power from 50 to 100 kW, is a cylindrical water-cooled jacket with a cover carrying graphite rod electrodes and inlet pipes for pulverized coal and gas. The plasma generator-reactor chamber is lined with graphite (thickness 0.02 m). The inner diameter of this chamber is 0.15 and its height is 0.3 m. The chamber is enclosed by an electromagnetic coil on the outside and bounded with a graphite diaphragm on the underside. The plasmatron (Fig. 1b) is fed by three-phase alternating current with a frequency of 50 Hz from a 200-kW electric power unit consisting of a three-phase transformer 11 regulated under load and inductive choke 10. Two electric phases are switched to the rod electrodes 1 (diameter 0.02 m), and the third phase is switched to the ring electrodes (diameter 0.15 m) (Fig. 1b). The distance between the rod electrodes and the ring electrode is 0.035 m. The three-phase alternating current arc burns between two rod electrodes and the rod and ring electrodes. It is localized in the electric arc zone of reactor 3 (height 0.08 m), enclosed from the outside by electromagnetic coil 4 (Fig. 1b).

The plasmatron power is determined by the formula

$$P_{\text{arc}} = \sqrt{3}IU$$

where I is the current strength and U is the voltage.

(*b*)

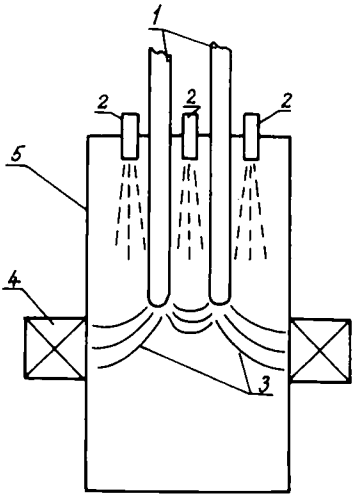

Fig. 1b. Plasma generator-reactor: 1, graphite rod electrodes; 2, piper for pulverized coal and gas; 3, zone of electrodischarge; 4, electromagnetic coil; 5, graphite round electrode.

The slag catcher is a water-cooled cylinder with a sampler inside.

The synthesis-gas oxidation chamber and the gasification-product cooling chamber are water-cooled steel cylinders.

The coal pulverization and pulverized coal feeding system consist of a ball mill and a star motor-operated feeder.

The steam feeding system consists of a hot-water boiler mounted on a weighing scale. The mixture of pulverized coal and gas is fed into the electric arc zone through piper 2 (Fig. 1b). The pulverized coal rate was determined by weighing within an error of 1.5%. The steam rate was varied within the range 0–10 kg/h. It was determined also by weighing within an error of 3%. The nitrogen flow rate through the coal pulverization ejectors was measured by a rotameter within an error of 2%. After completing the experiment, all the units were thoroughly cleared of the condensed phase, which was weighed to determine the mass of the solid residue in the coal conversion process.

The yield of gaseous products was measured with an orifice plate at the outlet of synthesis-gas oxidation chamber 3 (Fig. 1a).

Gas to be analyzed was taken into vessels 8 (see Fig. 1a) directly from the reactor arc chamber through a water-cooled probe. A special device was used for mechanical cleaning of the probe channel to prevent clogging up the channel with solid particles. The time for taking 50-ml samples did not exceed 10 min.

The gas was subjected to chromatographic analysis by the dynamic sampling and control method. The composition of the solid residue was examined by chemical and X-ray phase analyses.[8,9]

All the plant units were subjected to calorimetric measurements.

The water temperature was measured by thermocouples (Chromel–Copel) within an absolute error of 0.2°. The relative error was about 2%. The overall error in calorimetric measurements of heat flows was 6–10%.

The temperature of the reactor wall and the graphite diaphragm was measured by standard tungsten–rhenium thermocouples. The temperature correction for radiation from the thermocouple junction 10^{-3} m in diameter does not exceed 50°. The gas temperature in the reactor was not measured. Instead, the mean mass temperature of reagents was calculated from the material and heat balances of the plasma reactor.

2.2. Experimental Procedures

Coal conversion was carried out according to the following procedures. An arc was fired between the rod and ring electrodes by blasting a wire. Then pulverized coal from the star feeder bin was fed through two ejectors, mounted on the reactor cover, to the rod electrode ends. By means of the

carrier gas (nitrogen or synthesis gas), also fed through the ejectors, pulverized coal was uniformly distributed over the cross-section of the electric arc zone. The vapor was supplied axially through the two pipes on the reactor cover. After mixing, the vapor–pulverized coal mixture entered the arc discharge zone and was heated to high temperatures by the electric arc rotating in the magnetic field, thus producing a two-phase plasma flow where the coal gasification process basically occurred. The solid residue produced in the process was withdrawn through the diaphragm into the slag catcher. The gaseous products were fed through gas and slag separation chamber 2 into oxidation chamber 3, where carbon oxide and hydrogen were oxidized (Fig. 1a). Gaseous oxidation products were fed through the orifice plate, intended for measuring the off-gas flow rate, into cooling chamber 4 in which off-gases were cooled and cleaned of solid particles by means of a water spray. The cleaned and cooled gases were drained into the ventilation system.

The duration of the experiments was varied from 0.5 to 1.75 h depending on specific tasks.

In the course of the experiments material and heat flows were controlled and measured in all the apparatus units, which was necessary for calculating material and heat balances. Specifically, the following parameters were recorded: electric power, flow rates of water vapor, coal, nitrogen, off-gases, and cooling water, temperature under the reactor cover, temperatures of reactor walls, graphite diaphragm, and off-gases at the center of the orifice plate.

The material and heat balance equations assume the following form:

$$G_2 + G_3 + G_4 + G_5 = G_6 + G_1 + G_7$$

$$P_{arc} + P_1 = P_2 + P_3 + P_4 + P_5 + P_6$$

where G_2, G_3, G_4, and G_5 are the flow rates of coal, water vapor, carrier gas for coal pulverization, and electrode graphite; G_6, G_1, G_7 are the mass rates of slag (solid residue), off-gases, and pulverized coal being removed, respectively; P_{arc} is the heat output of the arc, P_1 is the heat supplied in vapor at $T = 405$ K; the heat losses in the apparatus units are: P_2 in the reactor, P_3 in the gas and slag separation chamber, P_4 in the synthesis gas oxidation chamber, P_5 in the slag catcher, and P_6 is the heat carried away in the off-gas (Fig. 2a).

The arc heat output is determined by the electric power input. The heat input in vapor was calculated by the formula

$$P_1 = G_3 H_1$$

(*a*)

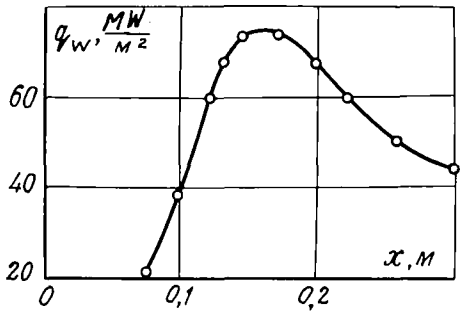

Fig. 2a. Variation of specific heat flow to wall g_w with increase in the reaction zone length.

where $H_1 = H^\circ_{405\,K} + \Delta H^\circ_{vap} = 0.05 + 0.63 = 0.68$ kWh/kg of vapor (H°_{vap} is the heat of vaporization).

The heat loss in the off-gases was determined from the off-gas temperature (T_6), flow rate (G_1), and composition obtained from the gas analysis. The measured temperatures, pressure, and composition of gases were fed into the ACTPA-3 program[10] and the specific enthalpy of the off-gases was computed at specified values of the parameters mentioned above. The gas mixture heat output was calculated according to the formula

$$P_6 = H_6 G_1$$

where $H_6 = \int_{300^\circ}^{T_6} C_{p.g}\, dT$ is the specific enthalpy of the gas mixture.

The specific power consumption Q_{sp} for coal gasification was determined from the formula[5]

$$Q_{sp} = J_{eq} - Z_{fs}(Q^d_s + J_{pc}) - Z_{ox}\Delta H^\circ_f(T_0)_{ox} \qquad (1)$$

where J_{eq} and J_{pc} are the total specific enthalpies of the reagents and products (coal + oxidizer) after gasification in the equilibrium state and of the products of coal combustion in air at a standard temperature $T_0 = 298.15$ K, Q^d_s is the highest heat of coal combustion on the dry mass, measured at the temperature T_0, $\Delta H^\circ_f(T_0)_{ox}$ is the standard heat of oxidizer formation, and Z_{fs} and Z_{ox} are the fractions of the total masses of solid fuel and oxidizing agent.

The degree of coal carbon gasification and the degree of sulfur conversion into the gas phase were determined from the carbon and sulfur content of the solid gasification products obtained from the results of the chemical analysis of samples. More particularly, ξ_c and ξ_s were calculated according to the following expressions[11]:

$$\xi_c = \frac{C_1 - C_2}{C_1} \cdot 100\%, \qquad \xi_s = \frac{S_1 - S_2}{S_1} \cdot 100\% \qquad (2)$$

Table I. Chemical Analysis of Brown Coals, mass %

Coal Number	A^d(%)	C	O	H	N	S	SiO_2	Al_2O_3	Fe_2O_3	CaO	MgO_2
1	12.7	60.87	20.33	3.88	1.43	0.79	6.23	2.68	1.30	2.0	0.49
2	26.8	548.54	18.33	3.63	0.78	1.87	15.40	7.85	2.05	0.8	0.65
3	48.1	33.60	8.52	6.50	0.88	2.40	25.82	16.13	1.73	0.41	0.46

where C_1, S_1 are the initial amounts of carbon and sulfur in the coal; C_2, S_2 are the final amounts of carbon and sulfur in the solid residue.

2.3. Results of Experiments

Finely ground brown coals from the Kansko-Achinsk (1), Turgay (2), and Podmoskovnyi (3) coal basins were used in the experiments. The sieve analysis of the feedstock showed that the maximum diameter of particles was less than 120 μm.

The ash content of the coals varied between 13 and 48%. Table I presents the chemical analysis of coals. The highest combustion heat of coal on the dry mass was 23,430, 18,140, and 16,130, kJ/kg for coals 1, 2, and 3, respectively.

Below, the coals from the basins mentioned above will be referred to by the numbers 1, 2, and 3 (cf. Table I.)

Figure 2a gives the specific heat flow to the wall (q_w), and Fig. 2b gives the temperature distribution in the apparatus units characteristic of the

(*b*)

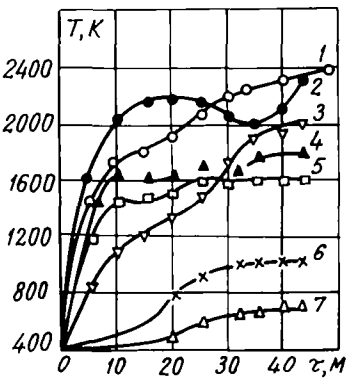

Fig. 2b. Variation of temperatures of gas phase and of apparatus units with time. (1-4) Temperature in the reactor wall height; (5, 6) gas temperatures at the reactor outlet and at the orifice plate center: (7) gas temperature after the cooling chamber.

gasification process, and the off-gas temperatures. As can be seen from Fig. 2b, the ring electrode temperature in the arc zone (curve 1) reaches 2400 K and the temperature of the wall at the end of the reaction zone (curve 4) reaches about 1800 K. The temperature of the gaseous gasification products at the reactor outlet is rather high, about 1600 K (curve 5). The off-gas temperature after the cooling chamber is about 700 K.

Measurements of the distribution of heat flows in different apparatus units (Fig. 3) indicated that on firing the arc and feeding the vapor-coal mixture into the reactor, steady-state heat condition was established in

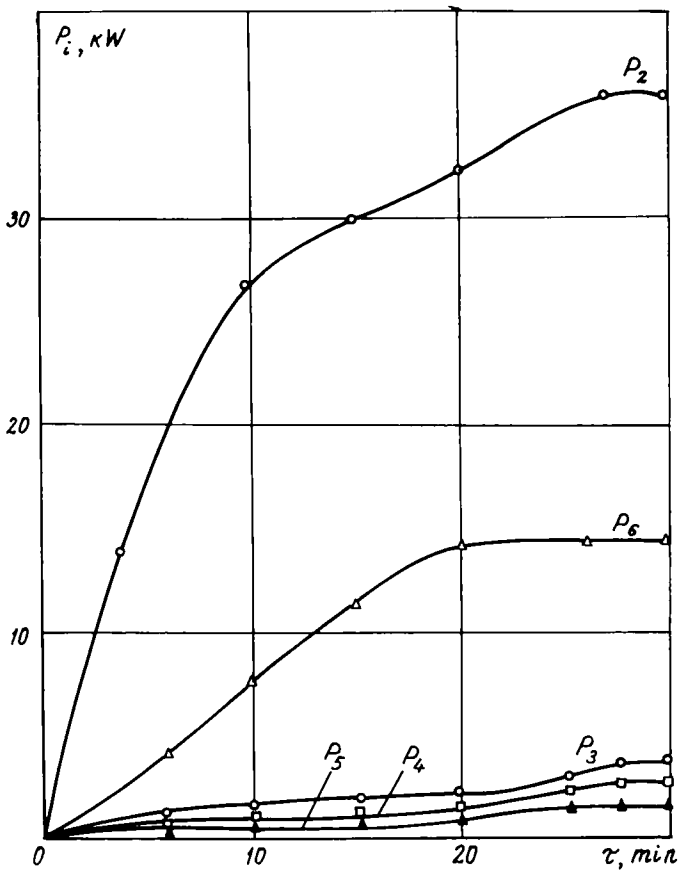

Fig. 3. Heat losses in the apparatus units: P_2, in the reactor; P_3, in the gas and slag separation chamber; P_4, in the synthesis gas oxidation chamber; P_5, in the slag catcher; P_6, heat carried away in the off-gas.

Table II. Material Balance

Input (kg/h)	Coal 1	Coal 2	Coal 3	Flow rate (kg/h)	Total 1	Total 2	Total 3
G_2	5.80	7.13	6.70	G_6	0.68	2.65	2.08
G_3	3.90	3.20	2.40	G_1	10.10	9.16	6.96
G_4	0.21	0.23	0.20	G_7	0.06	0.07	1.11
G_5	1.50	1.50	1.50	—	—	—	—
Total	11.41	12.06	10.80	Total	10.84	11.88	10.15

0.25–0.28 h. Following the establishment of the steady-state heat condition, gas and solid residue samples were taken for the gas and chemical analyses.

The material and heat balances for plasma gasification of coals 1, 2, and 3 are presented below for three representative experiments 1, 2, and 3, respectively (see Tables II and III).

The errors in the material balance for coals 1, 2, 3 are 5.1, 2.2, and 6.2%, respectively, which is within the limits of errors in the measurements of material flows.

The errors in the estimation of the heat balance are 7.8, 3.5, and 7.2% for coals 1, 2, and 3, respectively, which is also within the limits of relative errors in the measurements of heat flows.

The gas analysis results, averaged over the number of samples in each experiment, are presented in Table IV (for the indicated mean process temperature). As is evident from Table IV, in vapor gasification the hydrogen concentrations in the synthesis gas are always higher than the CO concentrations. The ratio H_2:CO varies in the range 1.14–1.38. The synthesis gas yield reaches a considerable value, from 84.7 to 85.7%. On substituting the recycled portion of the synthesis gas for the carrier gas nitrogen, the concentration of synthesis gas in the gas phase may increase up to 95–96%,

Table III. Heat Balance

Heat input (kW)	Coal 1	Coal 2	Coal 3	Heat removal (kW)	Total 1	Total 2	Total 3
P_{arc}	80.60	62.00	62.00	P_2	43.50	29.10	31.80
P_1	2.65	2.87	1.63	P_3	11.93	13.50	10.43
—	—	—	—	P_4	6.70	5.15	3.50
—	—	—	—	P_5	2.10	5.05	3.11
—	—	—	—	P_6	12.54	9.65	10.37
Total	83.25	64.87	63.63	Total	76.77	62.45	59.21

Table IV. Comparison between Experimental Calculated Data

Methods[a]	T (K)	$\gamma = G_3/G_2$	Content (vol. %) CO	H_2	N_2	ξ_c (%)	ξ_s (%)	Q_{sp} (kW h/k)
Experiment 1	3000	0.50	39.6	45.1	15.3	95.0	96.7	13.8
Calculation 1	2870		39.9	43.7	16.4	83.5	—	13.1
Experiment 2	3100	0.45	35.8	49.4	14.8	92.3	95.2	8.8
Calculation 2	3030		34.9	37.6	31.6	92.2	—	10.0
Experiment 3	3000	0.36	38.2	47.5	14.3	90.5	94.3	9.2
Calculation 3	2950		32.2	52.1	14.8	81.6	—	9.4

[a] Numbers of experiments and calculations correspond to the numbers of coal in Table I. Experimental temperature values correspond to mass-averaged values, and calculated values correspond to temperatures at the reactor outlet ($L_R = 0.3$ m).

and nitrogen in the gasification products will be represented only by the fuel nitrogen (4–5%).

On the basis of material and heat balances the parameters of the gasification process were obtained (Table IV). The mean temperature of the process for all the coals changed in a comparatively narrow range of 3000–3100 K. The mass ratio of the vapor and coal flow rates γ was varied between 0.36 and 0.67 kg/kg, increasing with increase of carbon content in the coals (Table I). The degree of coal gasification was 90.5–95.0%, and the degree of sulfur conversion to the gas phase was 94.3–96.7%. The correlation between ξ_c and ξ_s is evident from the tabulated data: with increase in the degree of gasification, the level of sulfur conversion into the gas phase also increases. Both of these values only slightly depend on the ash content in the fuels, which varies in a wide range from 13 to 48%. For instance, the degree of gasification changes comparatively little from 95 to 90.5% for coals 1 and 3 having equal temperatures (3000 K) and vastly different ash contents (13 and 48%) and γ ratios (0.67 and 0.36), though a trend to its increase with increase in surplus water vapor and decrease in ash content was observed for the coal types under study.

Note that the specific power consumptions given in Table IV are characteristic of the laboratory plasma reactor with a low thermal efficiency ξ equal to 46–53%. The experimental evidence points to the fact that with increase in ξ and decrease in mean temperatures of the process down to $T = 1800$–2000 K the specific power consumption Q_{sp} decreases, approaching the theoretically required values calculated by formula (1): 2.12 for coal 1, 2.26 for coal 2, and 2.75 for coal 3 ($\xi = 0.8$, $T = 2000$ K).

The results of X-ray phase analysis of the condensed gasification products show that carbosilicium (SiC) and two forms of ferrosilicium (FeSi

and Fe_5Si_3) in the crystalline state are present in the slag from the reactor and slag catcher, which confirms the possibility of reduction of the mineral part of oxides of lower-grade coal simultaneously with the production of synthesis gas with a heat of combustion of 10,000–12,000 kJ/nm^3.

Thus, experimental studies of brown-coal plasma gasification show that from lower-grade coals high-calorific synthesis gas can be produced which, after removal of hydrogen sulfide (concentration 0.7–0.8%), can be used as an ecologically clean fuel or for the synthesis of methanol.

3. MATHEMATICAL MODEL OF GASIFICATION OF FINELY DISPERSED COAL

The mathematical model of the coal gasification process describes a two-phase chemically reacting stream. The following chemical transformations are considered: formation of primary volatile products, conversion of evolved volatile products in the gas phase, and coke residue gasification reactions.

The process of high-temperature coal conversion is carried out usually at atmospheric pressure and temperatures of 1500–3000 K. The gas stream as a rule is strongly turbulized, and the temperature and velocity distributions are practically uniform along the reactor radius. The particle volume fraction is 10^{-3}–10^{-4} m^3/m^3.

Under these conditions, the interaction between particles may be neglected and, when modeling the processes, it is possible to use the results[12,13] obtained for single particles.

For the coal particle dimensions considered, convective heat transfer from gas to particle is a limiting stage as compared with heat transfer inside the particle,[14] and the temperature gradient inside the particle is small.[15,16] Isothermality in the case under consideration is also not disturbed in heterogeneous gasification reactions.[17]

The model described in this article considers a stream with polydisperse coal particles and the process of its heating with an electrical arc.

The following assumptions were made in the formulation of the model:[18–20]

(a) the bulk flow process is a steady-state, one-dimensional process;

(b) the equation of state of an ideal gas is assumed to hold;

(c) a homogeneous mixture of gas and particles is assumed at the reactor inlet;

(d) local heat transfer between the gas and the solids includes convective and conductive components;

(e) the temperature gradients within the particle are negligible, and the temperature is uniform throughout the particle;

(f) the heat of reaction of the solid-gas phase reaction affects the temperature of the solids only, while that of the gas-phase reaction affects the gas-phase temperature only;

(g) particle-particle interaction and solid-wall friction are neglected due to the dilute system;

(h) viscosity effects are appreciable only in the gas-solid phase interaction.

These assumptions make it possible to use ordinary differential equations, which substantially simplifies the computation of the process gas dynamics and still allows a detailed description of the process chemistry.

For the construction of a reliable mathematical model of polydisperse coal particle gasification, the set of equations must include equations for component concentrations (chemical kinetics equations) in conjunction with equations for gas and particle velocities and temperatures, respectively.

Recently, a mathematical model of such a type was reported.[18,19] The model describes the pyrolysis and gasification of monodisperse coal particles in a high-temperature gas stream.

The polydispersity of coal particles is accounted for by including in the equations a certain number of representative pulverized coal fractions chosen from coal particle size distribution by mesh analysis of coal powder after the mill.

Without loss of generality, we can assume that the components of the set are numbered as follows:

$i = 1, \ldots, n$ are gaseous components;
$i = n+1, \ldots, N$ are solid-state components;
$j = 1, \ldots, m$ are heterogeneous reactions;
$j = m+1, \ldots, M$ are gaseous reactions;
$l = 1, \ldots, L$ are fractions.

Then the set of equations takes on the following form:

Gas species balance

$$\frac{d_i}{dx} = \frac{f_i}{v_g} - \frac{c_i}{v_g}\frac{dv_g}{dx} - \frac{c_i}{S}\frac{dS}{dx}, \qquad i = 1, \ldots, n \tag{3}$$

Solid species balance

$$\frac{dc_{i,l}}{dx} = \frac{f_{i,l}}{v_{s,l}} - \frac{c_{i,l}}{v_{s,l}}\frac{dv_{s,l}}{dx} - \frac{c_{i,l}}{S}\frac{dS}{dx}, \qquad i = 1, \ldots, N;\ l = 1, \ldots, L \tag{4}$$

Constitutive equation

$$\frac{dv_{s,l}}{dx} = \frac{1}{M_{s,l}v_{s,l}} C_{D,l}\frac{\pi R_{s,l}^2 \rho_g (v_g - v_{s,l})|v_g - v_{s,l}|}{2}, \qquad l = 1, \ldots, L \tag{5}$$

Solid-phase energy balance

$$\frac{dT_{s,l}}{dx}=\frac{1}{C_{p,l}\rho_{s,l}v_{s,l}}\left(\sum_{j=1}^{m} Q_j W_j+4\pi R_{s,l}^2 N_l[\alpha_l(T_g-T_{s,l})+\varepsilon\sigma(T_w^4-T_{s,l}^4)]\right),$$

$$l=1,\ldots,L \tag{6}$$

Mixture momentum balance

$$\frac{d}{dx}\left(\left[\rho_g v_g^2+\sum_{l=1}^{L}\rho_{s,l}v_{s,l}^2\right]S\right)=-S\frac{dP}{dx}-\pi D F_W \tag{7}$$

Gas-phase energy balance

$$\frac{d}{dx}\left(\left[\rho_g v_g\frac{v_g^2}{2}+\sum_{l=1}^{L}\rho_{s,l}v_{s,l}\frac{v_{s,l}}{2}\right]S\right)+SC_{p,g}v_g\frac{dT_g}{dx}$$

$$=S\sum_{j=m+1}^{M} W_j Q_j+S\sum_{l=1}^{L} 4\pi R_{s,l}^2 N_l\alpha_l(T_{s,l}-T_g)+s\xi q_{\text{arc}} \tag{8}$$

Ideal gas law

$$P=R_g T_g\sum_{i=1}^{n} c_i \tag{9}$$

Gas residence time

$$\frac{d\tau_g}{dx}=\frac{1}{v_g} \tag{10}$$

Solid residence time

$$\frac{d\tau_{s,l}}{dx}=\frac{1}{v_{s,l}} \tag{11}$$

where $\alpha_1=(\lambda/2R_{s,l})Nu_l$; $N_l(x)=N_l^\circ[v_{s,l}^\circ S^\circ/v_{s,l}(x)S(x)]$; N_l is volume concentration of particles; $\sum_{i=1}^{n} c_i C_{p,i}=C_{p,g}$ is the effective heat capacity of the gaseous components; and $\sum_{i=n+1}^{N}\sum_{l=1}^{L} c_{i,l}C_{p,i}=C_{p,s}$ is the effective heat capacity of solid-state component fractions.

From Eqs. (7) and (8) we can get explicit terms for dv_g/dx and dT_g/dx:

$$\frac{dv_g}{dx}=\frac{b_1a_{22}-b_2a_{12}}{a_{11}a_{22}-a_{12}a_{21}} \tag{12}$$

$$\frac{dT_g}{dx}=\frac{b_2a_{11}-b_1a_{21}}{a_{11}a_{22}-a_{12}a_{21}} \tag{13}$$

where

$$a_{11} = \rho_g v_g - \frac{P}{v_g}, \qquad a_{12} = \frac{P}{T_g}, \qquad a_{21} = v_g C_{p,g}, \qquad a_{22} = \rho_g v_g^2$$

$$b_1 = -\frac{RT_g}{v_g} \sum_{i=1}^{n} f_i - v_g \sum_{i=1}^{n} \mu f_i - \sum_{l=1}^{L} \left(v_{s,l} \sum_{i=n+1}^{N} \mu f_{i,l} + \rho_{s,l} v_{s,l} \frac{dv_{s,l}}{dx} \right) - F_W + \frac{P}{S} \frac{dS}{dx}$$

$$b_2 = -\frac{v_g^2}{2} \sum_{i=1}^{n} \mu f_i + \sum_{j=m+1}^{M} W_j Q_j + \sum_{l=1}^{L} \times \left(-\frac{v_{s,l}^2}{2} \sum_{i=n+1}^{N} \mu f_{i,l} + \rho_{s,l} v_{s,l}^2 \frac{dv_{s,l}}{dx} + \sum_{l=1}^{L} 4\pi R_{s,l}^2 N_l \alpha_l (T_{s,l} - T_g) \right) + \xi q_{\text{arc}}$$

Let us consider some terms appearing in the equations of the system.

Term $C_{D,l}$ in Eq. (5), representing the drag coefficient of the particle moving under the action of Stokes force, takes on the form[20]

$$C_{D,l} = \begin{cases} 24/\mathrm{Re}_{s,l}(1 + 0.15\mathrm{Re}_{s,l}^{0.687}), & \mathrm{Re}_{s,l} < 1000 \\ 0.44 \quad , & \mathrm{Re}_{s,l} \geq 100 \end{cases}$$

where $Re_{s,l} = 2R_{s,l}|v_g - v_{s,l}|\rho_g/\eta$; $\eta = 2.71 \times 10^{-7} \cdot T_g^{0.719}$ is the empirical dependence of the dynamic viscosity coefficient of plasma-forming gas (water vapor) on its temperature; $\mathrm{Pr} = 1.48$ in the case of water vapor; $\eta = 3.66 \times 10^{-7} \cdot T_g^{0.690}$; $\mathrm{Pr} = 0.68$ if the plasma-forming gas is air.[21]

The Nusselt number was calculated from the empirical formula[22]

$$\mathrm{Nu}_l = 2 + 0.654 \cdot \mathrm{Re}_{s,l}^{1/2} \cdot Pr^{1/3}$$

The frictional force in Eq. (7) takes on the form[20]

$$F_W = \frac{f_g \rho_g v_g^2}{2D}$$

where the friction coefficient can be derived from the Blasius empirical

formula:

$$f_g = \frac{0.316}{\mathrm{Re}_w^{0.25}}, \qquad \mathrm{Re}_w < 100{,}000$$

and

$$\mathrm{Re}_w = \frac{D\rho v_g}{\eta}$$

The effects associated with Knudsen flow are small in the case under consideration. In addition, it should be noted that the effects associated with the evolution of volatile products have no appreciable influence on the motion of particles.[16] The values of λ appearing in the equations were calculated from the formula

$$\lambda = \frac{\eta C_{p,i}}{\mathrm{Pr}}$$

derived from the determination of Pr[23].

Individual values of the heat capacity of components were calculated on the basis of approximating polynomials, the values of which were taken from the automated data bank of ACTPA (automatic system of thermodynamic calculations).[10]

For complex hydrocarbons, the heat capacities and heats of formation were calculated from the values of the increments given in Ref. 24, and the ash heat capacities were taken from Refs. 25 and 26.

The thermal effects of all the reactions, except for the primary coal destruction reactions (1)-(6), were calculated from the heats of formation of compounds participating in the reactions.

The thermal effects of reactions of volatile matter evolution were determined from the difference between the effective and real heat capacities of coal.[25,26]

The thermal input of the arc is defined in the model as the difference between the arc electric power P_{arc} and the heat loss to the wall P_2 (see Fig. 3):

$$\Delta P = P_{\mathrm{arc}} - P_2, \qquad \Delta P / V = \xi q_{\mathrm{arc}},$$

where $\xi = (1 - P_2/P_{\mathrm{arc}})$ is the thermal efficiency of the plasma reactor. The arc electric power is expressed in terms of the heat loss to the wall:

$$P_2 = \pi D \int_0^{L_R} q_w(x)\, dx$$

where q_w is the specific heat flow to the wall of the plasma reactor (see Fig. 2a), and L_R is the plasma reactor length; this heat flow is approximated as

follows: $q_w = q_0 \exp(Bx + Cx^2)$, where B and C are normalization factors: $B = 0.116$, $C = -3.854 \times 10^{-3}$; x is the longitudinal coordinate.

The temperature of the wall along the reactor length was determined by a similar formula with the same coefficients:

$$T_W = T_0 \exp(Bx + Cx^2)$$

The values of q_0 and T_0 were chosen so that the heat loss to the wall and the wall temperature, measured during the experiment, could be best described.

It should be noted that during carbon oxidation heat release occurs on the surface of particles of different fractions, which is accounted for by the first term in Eq. (6).

To formulate the initial conditions for the system of equations, it is necessary to preset the values of the initial velocities and temperatures for gas and particles, the pressure at the reactor inlet, the reactor wall temperature, and the ratio of gas-to-solid mass flow rate.

Since the system of equations obtained is appreciably nonlinear and has a comparatively large dimension, it can be solved only with the use of numerical methods. The described model was realized as a 386-series computer program in FORTRAN-77. We used the modification of the program K-81 described in Ref. 27 and intended for the solution of stiff systems of chemical kinetics equations by Gear's method, with the addition of differential equations for velocities, temperatures, and residence times of gas and particles.

The model developed is distinguished by its detailed description of the kinetics of chemical reactions whose general scheme, along with the reactions of evolution of primary products, takes into account the reactions of their further transformations (Table V).

The first chemical stage of coal conversion in the plasma-chemical reactors is the evolution of volatile matter. It has been proved experimentally[28] that the composition of the primary products and the velocity of their evolution from coal practically do not depend on the temperature and composition of the plasma-forming gas. Therefore, this stage can be described by a single kinetic mechanism for various plasmachemical processes (e.g., pyrolysis, hydropyrolysis, gasification with water vapor).

Study of coals of different rank by FT-IR spectrometry showed that they differ in the concentration of functional groups.[29] Study of the evolution and decomposition of the functional groups by the same method and determination of the concentrations of the products formed (CH_4, H_2O, CO, CO_2, etc.) yielded the rates constants of evolution and decomposition of these functional groups and the formation rate of final products from them. It was found that the evolution rate constants of these groups for all

Table V. Kinetic Parameters of Reactions Included in the Mathematical Model[a]

Reaction[b]	Log A[c]	n	E/R (K)
(1) $[H_2]_s = H_2$	18.2	0	44.67
(2) $[H_2O]_s = H_2O$	13.9	0	25.86
(3) $[CO]_s = CO$	12.3	0	22.33
(4) $[CO_2]_s = CO_2$	11.3	0	16.40
(5) $[CH_4]_s = CH_4$	14.2	0	25.96
(6) $[C_6H_6]_s = C_6H_6$	11.9	0	18.80
(7) $C + H_2O = CO + H_2$	7.5	0	10.57
(8) $C + CO_2 = CO + CO$	11.6	0	21.62
(9) $C + O_2 = CO_2$	12.3	0	19.10
(10) $CH_4 + H = CH_3 + H_2$	11.1	0	5.98
(11) $CH_4 + OH = CH_3 + H_2O$	0.5	3.1	1.00
(12) $CH_4 + M = CH_3 + H + M$	14.2	0	44.46
(13) $CH_4 + O = CH_3 + OH$	10.2	0	4.63
(14) $CH_3 + H_2O = CH_4 + OH$	9.8	0	12.48
(15) $CH_3 + H_2 = CH_4 + H$	9.7	0	5.74
(16) $CH_3 + M = CH_2 + H + M$	13.3	0	46.83
(17) $CH_3 + O_2 = CH_3O + O$	10.7	0	14.58
(18) $CH_3 + OH = CH_2O + H_2$	9.6	0	0
(19) $CH_3 + O = CH_2O + H$	11.1	0	1.01
(20) $CH_3O + M = CH_2O + H + M$	10.7	0	18.83
(21) $CH_2O + M = HCO + H + M$	13.5	0	40.75
(22) $HCO + M = H + CO + M$	11.2	0	9.55
(23) $O_2 + M = O + M$	12.7	0	57.85
(24) $H_2 + M = H + H + M$	11.3	0	48.29
(25) $H + O_2 = O + OH$	11.3	0	8.45
(26) $H + H_2O = H_2 + OH$	11.0	0	10.22
(27) $H_2 + O = H + OH$	7.3	1.0	4.48
(28) $H_2O + M = H + OH + M$	13.3	0	52.8
(29) $H_2O + O = OH + OH$	10.5	0	9.20
(30) $CO + OH = CO_2 + H$	4.1	1.3	−0.41
(31) $CO_2 + H = CO + OH$	6.2	1.3	10.87
(32) $CO + O + M = CO_2 + M$	9.8	0	2.06
(33) $C_2H_2 + M = C_2H + H + M$	11.0	0	57.34
(34) $C_2H_2 = C + C + H_2$	6.0	0	15.07
(35) $C_2H_2 + O_2 = HCO + HCO$	9.6	0	14.08
(36) $C_2H_2 + H = C_2H + H_2$	11.3	0	9.55
(37) $C_2H_2 + OH = CH_3 + CO$	9.1	0	0.24
(38) $C_2H_2 + O = CH_2 + CO$	10.8	0	2.00
(39) $CH_2 + H_2O = CH_2O + H_2$	11.0	0	1.87
(40) $CH_2 + O_2 = HCO + OH$	11.0	0	1.87
(41) $C_2H + O_2 = HCO + CO$	10.0	0	3.52
(42) $C_2H + H_2O = CH_3 + CO$	9.1	0	0.24
(43) $C_6H_6 = C_2H_2 + C_2H_2 + C_2H_2$	12.0	0	42.76
(44) $OH + OH = H_2O + O$	9.5	0	0.55
(45) $H + OH + M = H_2O + M$	10.6	0	0
(46) $H + H + M = H_2 + M$	9.6	0	0
(47) $CH_2 + OH = HCO + H_2O$	10.5	0	0.76
(48) $H + OH = H_2 + O$	9.8	3.52	
(49) $H_2 + OH = H_2O + H$	11.4	0	5.03

[a] The temperature dependence of rate constants is governed by the Arrhenius equation $k_i = A_i \exp(-E_i/RT)T^n$.

[b] Equations (1)-(6) are the devolatilization reactions.

[c] Dimensions of A_i are s^{-1} for first-order reactions and liter $mol^{-1}\ s^{-1}$ for second-order reactions.

the coals are equal to a sufficient degree of accuracy. For many coals, no data on the concentration of different functional groups in them are available. In such cases it may be considered, to a first approximation, that the composition and total quantity of the evaluated primary products of coal destruction correspond to those determined by standard methods of analysis.

With the particle heating rates realized in plasma and with the particle dimensions that are usually used (10^{-4}-10^{-5} m), the coal decomposition process proceeds as a first-order reaction.

Table V lists the values of the kinetic parameters, taken from Ref. 30, for the water, hydrogen, carbon oxide and dioxide, ethylene methane, and tar production reactions that were used in the model to describe the kinetics of the first stage, i.e., thermal devolatilization of coal [reactions (1)-(6)].

Further transformations of primary products are described by reactions of radical (10)-(49) in Table V, the rate constants of which are taken from Ref. 31.

The interactions between the coke residue and water vapor, oxygen and carbon dioxide [reactions (7)-(9)] are the rate-limiting stages of the process. The rate constants of these stages are taken from Ref. 19.

4. COMPARISON OF EXPERIMENTAL AND CALCULATED DATA

The calculation of the coal gasification processes was performed for flow rates of coal G_2 and water vapor G_3, and electric power of arc P_{arc} used in the experiments (see Tables I and II). The following particle size distribution was used in the calculation:

Fraction 1: $r_s = 5.0$ μm, 10.0%

Fraction 2: $r_s = 15$ μm, 20.0%

Fraction 3: $r_s = 30$ μm, 40.0%

Fraction 4: $r_s = 50$ μm, 20.0%

Fraction 5: $r_s = 60$ μm, 10.0%

Comparison between the calculation results and the experimental data (Table IV) shows that the calculated values of the gas temperature at the reactor outlet and the mean temperatures determined experimentally agree within an accuracy of ±100°. There is also practically complete agreement in the specific power consumption (Q_{sp}). According to the experimental and calculated data, the main gaseous products of the reactions are H_2 and CO, the calculated and experimental values of the H_2:CO ratios being similar. Carbon dioxide and light and heavy hydrocarbon are converted

almost completely into H_2 and CO in the reaction zone. In this sense, the compositions of the plasma-chemical coal gasification products differ considerably from the compositions obtained by conventional gasification methods: the carbon dioxide content in the latter case often exceeds 10%. The absence of carbon dioxide in the plasma-chemical coal gasification products makes possible their use as reducers in metallurgy, for example. The calculated values of the coal carbon conversion level ξ_c are substantially lower (by 9–13%) than those found in the experiment. Since the residual content of water vapor in the reaction products is small (for example, 3.6 and 0.89% for gasification of coals 2 and 3, respectively), the coal gasification level observed in the experiments cannot be achieved by reactions with water vapor only. Under the conditions of plasma-chemical gasification, the coal particles (especially the finest fractions) appear to be heated to such high temperatures that promote the reduction of the oxides of the mineral part of coal by carbon. This assumption is supported by the detection by the X-ray phase analysis of silica and iron carbides in the solid residues. Thus, the model should include reactions of this type.

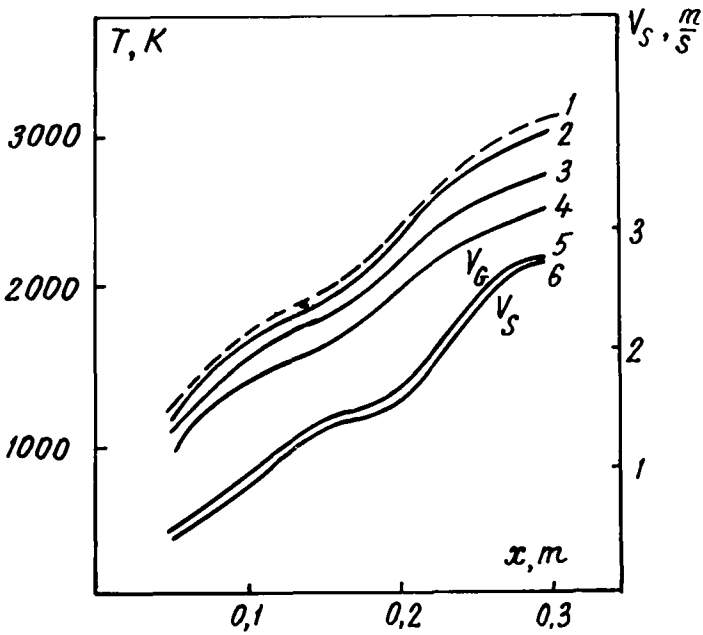

Fig. 4. Variation of temperature (1–4) and of gas and particle velocities (5–6) with increase in the reaction zone length in the process of gasification of coal 1. (1) Gas temperature; (2, 3, 4) temperatures of particles of fractions 1, 3, and 5, respectively; (5) gas velocity; (6) velocity of particles of fraction 5.

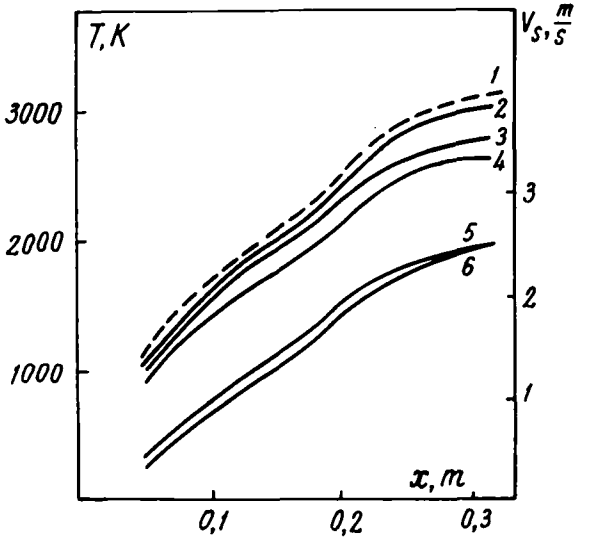

Fig. 5. Variation of temperature (1-4) and of gas and particle velocities (5-6) with increase in the reaction zone length in the process of gasification of coal 2. (1) Gas temperature; (2, 3, 4) temperatures of particles of fractions 1, 3, and 5, respectively; (5) gas velocity; (6) velocity of particles of fraction 5.

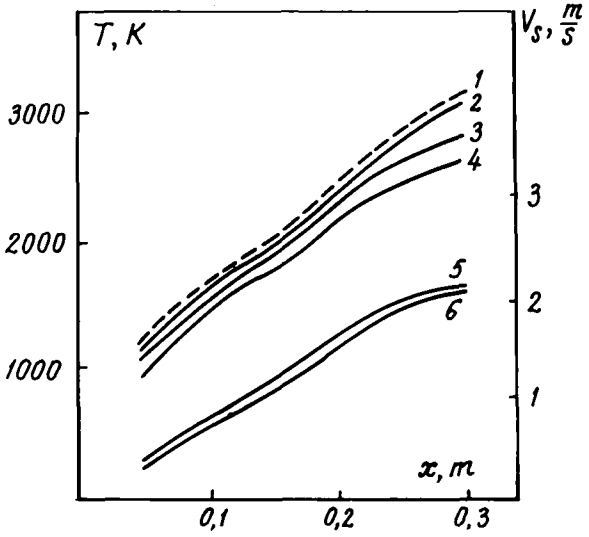

Fig. 6. Variation of temperature (1-4) and of gas and particle velocities (5-6) with increase in the reaction zone length in the process of gasification of coal. (1) Gas temperature; (2, 3, 4) temperature of particles of fractions 1, 3, and 5, respectively; (5) gas velocity; (6) velocity of particles of fraction 5.

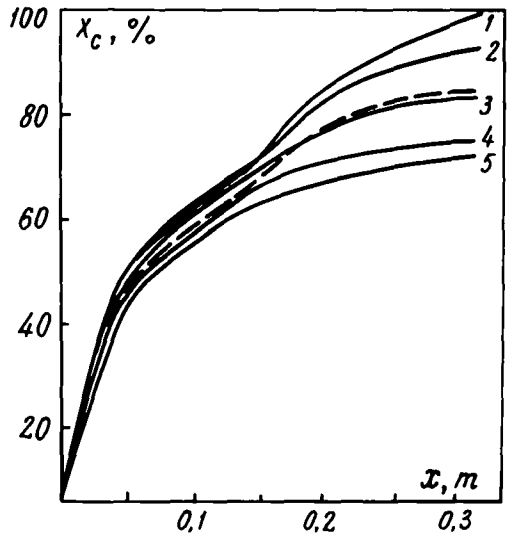

Fig. 7. Coal 1 particle conversion level as a function of the reaction zone length. (1-5) Conversion levels of organic matter of coal of fractions 1-5, respectively; dashed curve—total conversion level of organic matter of coal.

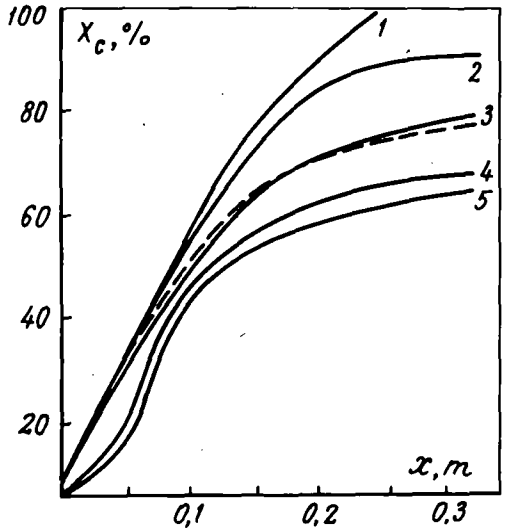

Fig. 8. Coal 3 particle conversion level as a function of the reaction zone length. (1-5) Conversion levels of organic matter of coal of fractions 1-5, respectively; dashed curve—total conversion level of organic matter of coal.

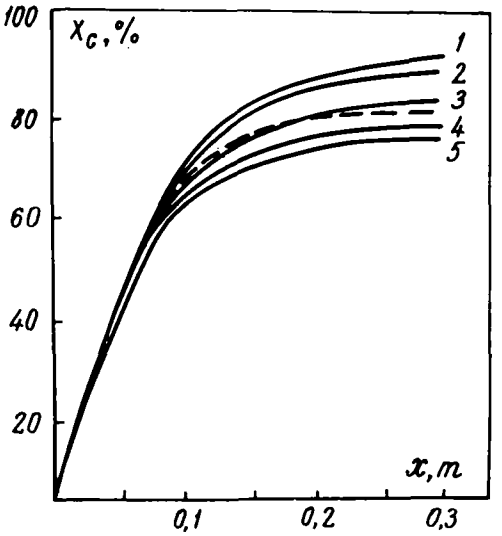

Fig. 9. Coal 3 particle conversion level as a function of the reaction zone length. (1-5) Conversion levels of organic matter of coal of fractions 1-5, respectively; dashed curve—total conversion level of organic matter of coal.

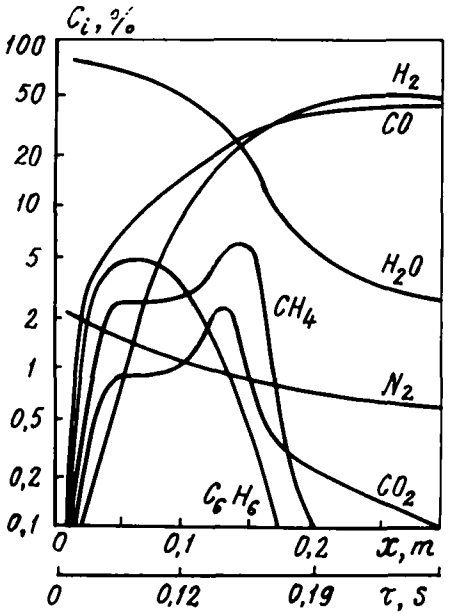

Fig. 10. Concentration variation of gaseous products of coal 1 gasification process with increase in the reaction zone length.

It is possible to calculate the curves of particle and gas temperatures and velocities, carbon conversion level, and product composition against the reactor length using the mathematical model (see Figs 4-12).

The patterns of the particle and gas temperature variation for the three different coals are similar: they increase with reactor length, the temperatures of fraction 1 particles exceeding the temperatures of fraction 5 particles by 400-500 K, and the gas temperature being higher than the temperature of fraction 1 particles by 50-90 K. The velocities of gas and particles differ slightly: by less than 5% in the case of the smallest and largest particles (Figs. 4-6).

The carbon conversion levels for particles of different size differ considerably (Figs. 7-9): in the gasification of coals 1 and 2, carbon of fraction 1 particles at the reactor outlet is converted completely, while the conversion of carbon of fraction 5 particles constitutes 63-70%. The total conversion of carbon in both cases is close to 80%. In the gasification of coal 3 the complete conversion of small particles cannot be achieved, yet the total

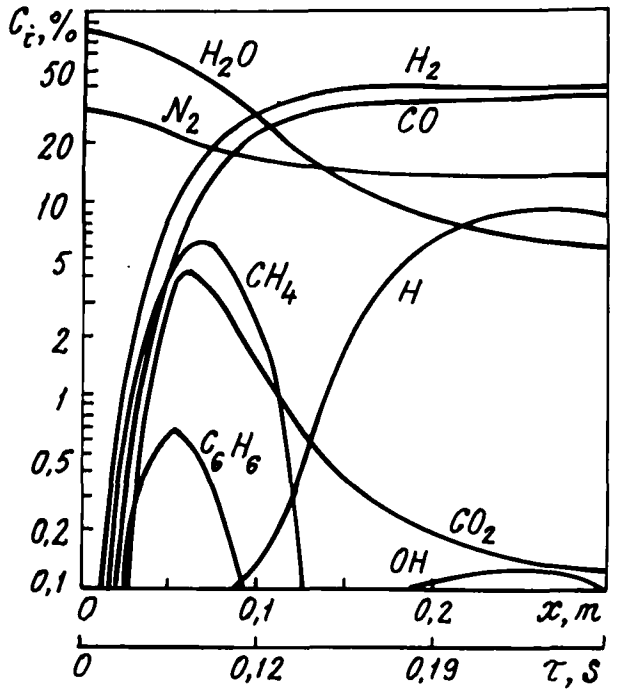

Fig. 11. Concentration variation of gaseous products of coal 2 gasification process with increase in the reaction zone length.

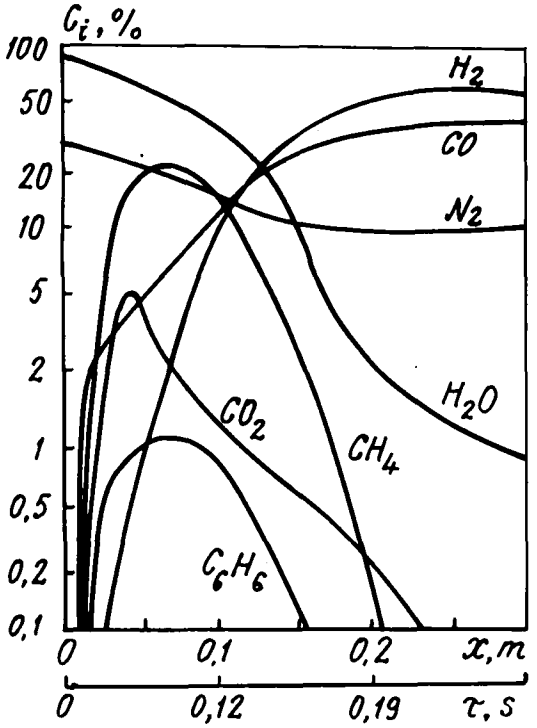

Fig. 12. Concentration variation of gaseous products of coal 3 gasification process with increase in the reaction zone length.

conversion of coal carbon in the latter case is also close to 80%. The residual content of water vapor in the gas mixture in the conversion of coals 1, 2, and 3 is 6.2, 3.6, and 0.89% (by volume), respectively. Thus, the incompleteness of coal carbon gasification is accounted for by the deficiency of water vapor in the system.

The variation of product composition with reactor length shows common trends: hydrogen and carbon oxide contents increase, while those of methane, carbon dioxide, and benzene drop practically to zero at the reactor outlet (Figs. 10-12).

5. CONCLUSIONS

We have studied the process of vapor gasification of various coals in a plasma reactor and developed a mathematical model describing the conversion of the polydisperse pulverized coal stream in a reactor of this type.

Comparison between the experimentally obtained data and the calculation results shows a satisfactory agreement between them and confirms the possibility of predicting the parameters essential for practice: reaction zone length, specific power consumption, synthesis gas yield, the mixture composition of the initial process, and others.

The calculations also give useful information on some characteristics of the process that are difficult to obtain experimentally, in particular the velocities, temperatures, and degrees of carbon conversion of coal particles of different size.

7. NOMENCLATURE

c_i —volume concentration of components (kmol m^{-3})
x —longitudinal coordinate (m)
f_i —source members, determined by variation of the ith component due to chemical reactions in unit volume in unit time (kmol m^{-3} s^{-1})
v —velocity (m s^{-1})
M_s —ash mass in one particle (kg)
C_D —particle drag coefficient
π —3.14
r_s —particle radius (m)
d —particle diameter (m)
ρ —density (kg m^{-3})
C_p —heat capacity of components (J mol^{-1} K^{-1})
Q_j —thermal effect of reaction (J $kmol^{-1}$)
E_j —activation energy of reaction
N_l —volume concentration of particles of the lth fraction (m^{-3})
T —temperature (K)
ε —emissivity factor of coal particles
σ —5.67×10^{-8}, blackbody emissivity coefficient (W m^{-2} K^{-4})
P —pressure (Pa)
S —reactor cross section (m^2)
D —reactor diameter (m)
V —reactor volume (m^3)
L_R —reactor length (m)
F_W —friction force on the wall (N)
f_g —friction coefficient
τ —residence time (s)
Nu —Nusselt number
Re —Reynolds number
Pr —Prandtl number
λ —thermal conductivity of gas (J m^{-1} s^{-1} K^{-1})

R —8.3×10^3, universal gas constant (J kmol K^{-1})
μ_i —molecular mass of component (kg $kmol^{-1}$)
η —dynamic viscosity coefficient of gas (kg m^{-1} s^{-1})
ξ —thermal efficiency of plasma reactor
q_{arc} —specific heat flow from arc (W m^{-3})
P_1 —heat supplied in vapor at $T = 405$ K (W)
P_2 —heat loss to wall (W)
P_3 —heat loss in the gas and slag separator chamber (W)
P_4 —heat loss in the synthesis gas oxidation chamber (W)
P_5 —heat loss in the slag catcher (W)
P_6 —heat carried away in the off-gas (W)
ΔP —heat input of arc (W)
P_{arc} —electric power of arc (W)
Q_{sp} —specific power consumption (kw Hr kg^{-1})
d_w —specific heat flow to wall (W m^{-2})
ξ_c —degree of carbon gasification (%)
ξ_s —level of sulfur conversion into gas phase (%)

7. INDICES

dif —refers to diffusion
s —refers to particle
W —refers to reactor wall
g —refers to gas phase
i —ordinal number of component:
$i = 1, \ldots, n$—gas components;
$i = n+1$—ash (mineral components of coal);
$i = n+2$—coal carbon;
$i = n+3, \ldots, N$—solid-state components evolved into gas phase on coal particle heating
j —ordinal number of chemical reaction:
$j = 1, \ldots, m$—heterogeneous reactions
$j = n+1, \ldots, M$—gaseous reactions
l —ordinal number of fraction
N —number of components
M —number of reactions
L —number of fractions

REFERENCES

1. D. Bittner, H. Bauman, C. Peucker, J. Klein, and H. Juntgen, *Erdol Kohle, Erdgas, Petrochem.* **34**, 237 (1981).
2. J. G. Wragg, M. A. Kaleel, and C. S. Kim, *Coal Process. Technol.* **6**, 186 (1980).

3. E. A. Kolobova, *Khim. Tverd. Topl.*, No. **2**, 91 (1983).
4. H. Herlitz and S. Santen, *Chem. Stosow.* **28**, 49 (1984).
5. V. E. Messerle, Z. B. Sakipov, and B. G. Trusov, *Izv. Sib. Otd. Akad Nauk SSSR, Ser. Tekh. Nauk*, No. **18**, 95 (1988).
6. Z. B. Sakipov, V. E. Messerle, Sh. Sh. Ibrayev, *et al.*, *Khimi. Vys. Energ.* **20**, 61 (1986).
7. Z. B. Sakipov, V. E. Messerle, Sh. Sh. Ibrayev, and V. P. Riabinin, Abstracts of Proc. of the 9th All-Union Conference on Low-Temperatures Plasma Generators, ILIM, Frunze, (1983), p. 364.
8. USSR State Standard GOST 10533-72: Brown Coal, Anthracite, Rock, Oil Shale, and Peat, Methods of Chemical Analysis of Ash.
9. American Society for Testing and Materials, Baltimore (1963).
10. G. B. Siniarev, N. A. Vatolin, B. G. Trusov, and G. K. Moiseev, *Computer Applications in Thermodynamic Calculations of Metallurgical Processes*, Nauka, Moscow (1982).
11. M. I. Vdovenko, Sh. Sh. Ibrayev, V. E. Messerle, *et al.*, *Plasma Gasification and Pyrolysis of High-Grade Coal*, ENIN, Moscow (1987), p. 59.
12. Z. R. Gorbis, *Heat Transfer and Hydrodynamics of Disperse Scvoznikh Flows*, Energia, Moscow (1970).
13. Z. F. Chuhanow, *Int. J. Heat Mass Transfer* **14**, 337 (1971).
14. H. Reidelbach, and J. Algermissen, Proceedings of the 13th Intersociety Energy Conversion Engineering Conference, Vol. 1, Society of Automotive Engineers (1978).
15. K. M. Sprouse, *AIChE J.* **26**, 964 (1980).
16. V. I. Babii and Yu. K. Kuvaiev, *Combustion of Coal Dust and Calculation of the Coal Dust Flame*, Energoatomizdat, Moscow (1986).
17. J. M. Thomas and W. J. Thomas, *Introduction to the Principles of Heterogeneous Catalysis*, Academic Press, London (1967).
18. R. A. Kalinenko, A. A. Levitskiy, Yu. A. Mirokhin, and L. S. Polak, *Kinet. Katal.* **28**, 723 (1987).
19. E. S. Golovina, R. A. Kalinenko, A. A. Levitskiy, Yu. A. Mirokhin, L. S. Polak, and O. S. Yusim, *Fiz. Goren. Vzryva* **5**, 88 (1988).
20. A. Goyal and D. Gidaspow, *Ind. Eng. Chem. Process Des. Dev.* **21**, 611 (1982).
21. N. B. Vargaftik, *Handbook of Thermophysical Properties of Gases and Liquids*, Nauka, Moscow (1972).
22. L. D. Smoot and D. J. Pratt, *Pulverized Coal Combustion and Gasification*, Plenum Press, New York (1979).
23. D. A. Frank-Kamenetskii, *Diffusion and Heat Transfer in Chemical Kinetics*, Nauka, Moscow (1967).
24. S. W. Benson, *Thermochemical Kinetics*, Wiley, New York, London (1976).
25. A. A. Agroskin, V. B. Gleibman, E. I. Goncharov, and V. P. Yakunin, *Koks Khim.* **2**, (1974).
26. A. A. Agroskin, E. I. Goncharov, L. V. Lovetskiy, L. A. Makeev, N. S. Griaznov, and V. V. Mochalov, *Koks Khim.* **11**, 1 (1968).
27. L. S. Polak, M. Ya. Goldenberg, and A. A. Levitskii, *Computational Methods in Chemical Kinetics*, Nauka, Moscow (1984).
28. H. J. Beiers, H. Bauman, D. Bittner, and I. Klein, Intern. Symp. on Plasma Chemistry, Eindhoven, Preprint, Paper No. B-2-2 (1985), p.232.
29. P. R. Solomon, D. J. Hambeln, R. M. Carangelo, and J. L. Krause, 19th Symp. Intern. Combustion, Pittsburgh (1982), p. 1139.
30. F. Kayihan and G. V. Reklaitis, *Ind. Eng. Chem. Process Des. Dev.* **19**, 15 (1980).
31. C. K. Westbrook, F. L. Dryer, K. P. Schug, 19th Symp. Intern. Combustion, Pittsburgh (1982), pp. 153-156.